Vol. 04, Iss. 4 (2026) 427-435, DOI: 10.61552/JME.2026.04.001

JME

Journal of Materials and Engineering

www.jme.aspur.rs

Research article

Effects of Rapid Thermal Annealing on Structure, Surface Roughness, and Adhesion Strength of Nitrogen-Doped Tetrahedral Amorphous Carbon Thin Films with Different Nitrogen Contents

Nay Win Khun[a,b,*], Adrian Wei-Yee Tan[c]

[a]*School of Mechanical and Aerospace Engineering, Nanyang Technological University, 50 Nanyang Avenue, Singapore 639798, Singapore,*
[b]*Institute of Microelectronics and Optoelectronics, Faculty of Electronics and Information Technology, Warsaw University of Technology, Koszykowa 75, 00-662 Warszawa, Poland,*
[c]*Smart Manufacturing and Systems Research Group (SMSRG), University of Southampton Malaysia, Iskandar Puteri 79100, Johor, Malaysia.*

Keywords:

taC thin films
N doping
Annealing
Structure
Adhesion Strength

* Corresponding author:

Nay Win Khun
E-mail: khunnaywin@gmail.com

Received: 10 March 2026
Revised: 30 April 2026
Accepted: 1 June 2026

A B S T R A C T

Nitrogen-doped tetrahedral amorphous carbon (taC:N) thin films with varying nitrogen concentrations were synthesized on silicon (Si) substrates using a filtered cathodic vacuum arc (FCVA) deposition process. Then, they were annealed at 200 ˚C for 2 minutes to study the effects of rapid thermal annealing (RTA) on their structure, surface roughness, and adhesion strength. It was found that the increased N content or the annealing increased the graphitization of the taC:N thin films, which was responsible for their increased surface roughness. The adhesion strength of the taC:N thin films increased with their increased N contents or the annealing as a result of their degraded sp^3-bonded cross-linking networks with the increased number of sp^2 bonds, N aggregates, and graphitic phases. It was concluded that changes in the structure, surface roughness, and adhesion strength of the taC:N thin films were apparently related to their N contents or the annealing.

© 2026 Journal of Materials and Engineering

1. INTRODUCTION

Diamond-like carbon (DLC) is a metastable amorphous carbon consisting mainly of a mixture of sp^3 and sp^2 bonds [1,2]. DLC thin films possess a remarkable combination of superior properties, including high electrical resistivity, exceptional hardness, low friction, excellent wear resistance, strong corrosion resistance, chemical inertness, and

biocompatibility. These attributes render them highly valuable for diverse industrial applications [3].

DLC thin films can be produced by physical (PVD) and chemical (CVD) vapour deposition techniques. Among PVD methods, the FCVA deposition technique can generate a plasma with highly energetic C species, which can penetrate a growing film and fill in pinholes to produce highly dense taC thin films [2]. Therefore, taC thin films possess the highest amount of sp^3 bonds, which is responsible for their highest mechanical strength and wear resistance, among various DLC thin films. However, the FCVA deposition technique induces high residual stress in taC thin films, which greatly limits their adhesion strength and, thereby, their film thickness [2,4,5]. Since thick films with strong adhesion strength are demanded by mechanical components or systems operating in harsh environments for their durability and long service life, it has been an important topic for researchers to improve the adhesion strength of taC thin films for several decades [2,4,5].

The incorporation of N atoms in taC thin films is a potential way to improve their adhesion strength by relaxing their residual stress [2,5]. However, the high N content degrades the mechanical strength and corrosion resistance of taC:N thin films, so it is necessary to optimize their N contents in order to make a balance between these properties based on their desired properties. Besides, not many studies on the effects of N doping on the adhesion strength of taC:N thin films have been found in the literature, which indicates that it is still necessary to comprehensively investigate their adhesion strength with respect to their N contents.

Annealing taC thin films is also another possible method to improve the adhesion strength of taC thin films because annealing degrades their rigid sp^3-bonded cross-linking structures, which are responsible for their high residual stress, with the increased number of sp^2 bonds in their C matrixes [6,7]. However, annealing process parameters are always complicated with metastable taC thin films, so it does not always give an improvement in their adhesion strength because of several problems, such as degassing, thermal mismatch between the film and substrate, and so on [8]. It is, therefore, necessary to optimize annealing process parameters to promote the adhesion strength of taC thin films. However, reports on the adhesion strengths of taC:N thin films with the annealing treatment are rare in the literature. It deserves to investigate the structure and adhesion strength of annealed taC:N thin films with different N contents to understand the combined effects of N content and annealing on their adhesion strength, which has not been widely reported in the literature yet.

In this study, the taC:N thin films with different N contents were prepared using a FCVA deposition technique and then annealed at the optimized temperature of 200˚C for 2 minutes to investigate the effects of RTA on their structure, surface roughness, and adhesion strength with respect to their different N contents [8].

2. EXPERIMENTAL DETAILS

2.1 Sample preparation

A nanofilms FCVA deposition system was used to deposit the taC:N thin films on p-type Si substrates (111) by varying the N_2 gas flow rate for their different N contents. A graphite target of ≥99.95% C was used as the C source. Table 1 shows the detailed deposition process parameters of the taC:N thin films.

Table 1. Deposition process parameters of taC:N thin films.

N_2 flow rate (sccm)	0.5	3	5	10	20
Working pressure (Torr)	2.8×10^{-6}	3.5×10^{-5}	5×10^{-5}	9.7×10^{-5}	1.9×10^{-4}
Bias (V)	1500				
Film thickness (nm)	100				

A Jipelec Jetfirst 100 RT processor was used to anneal the taC:N thin films with different N contents in a nitrogen environment, which was supplied by nitrogen gas at 2,000 sccm, at a temperature of 200˚C for 2 minutes. The temperature was ramped at 25˚C/s and then cooled down at 6˚C/s.

2.2 Characterization

The X-ray photoelectron spectroscopy (XPS, Kratos) attached with an X-ray source of a monochromatic Al K_α line ($h\upsilon$ = 1486.71 eV) was applied to measure the elemental compositions and chemical bonding structures of the taC:N thin films.

The bonding structures of the taC:N thin films were characterized by micro-Raman spectroscopy (Renishaw RM1000), which had a He-Ne laser of 632 nm. Raman data were averaged by five random measurements on each sample surface.

The atomic force microscopy (AFM, Digital Instrument, S-3000), which was attached with a tapping mode Si_3N_4 cantilever, was applied to capture the surface topographies of the taC:N thin films. The average value of arithmetic mean roughness (R_a), average maximum peak height (R_{pm}), and average maximum valley depth (R_{vm}) were determined from five random measurements on each sample surface.

A diamond stylus of 15 μm in radius attached to a micro-scratch tester (Shimadzu SST-101) was dragged down onto the taC:N thin film surfaces under progressive loading at room temperature (RT ~ 22–24˚C) to evaluate their adhesion strength, which was averaged by five random measurements per sample. The scan amplitude and frequency, scratch rate, and down speed were 50 μm, 30 Hz, 10 μm/s, and 2 μm/s, respectively.

The surface morphologies of the taC:N thin films were observed using scanning electron microscopy (SEM, JEOL-JSM-5600LV).

3. RESULTS AND DISCUSSION

Figure 1 presents the surface chemical composition variations in taC:N thin films deposited without and with RTA at 200°C for 2 minutes, analyzed against increasing N_2 gas flow rates. For non-annealed (as-deposited) taC:N films, the surface nitrogen concentration rises from 0.54 at.% to 5.29 at.% (9.8 times increase) as the N_2 flow rate escalates from 0.5 to 20 sccm.

The increased deposition pressure associated with the increased N_2 gas flow rate increases the concentration of N species in the deposition chamber during the film deposition, resulting in the increased N content of the taC:N thin films [9].

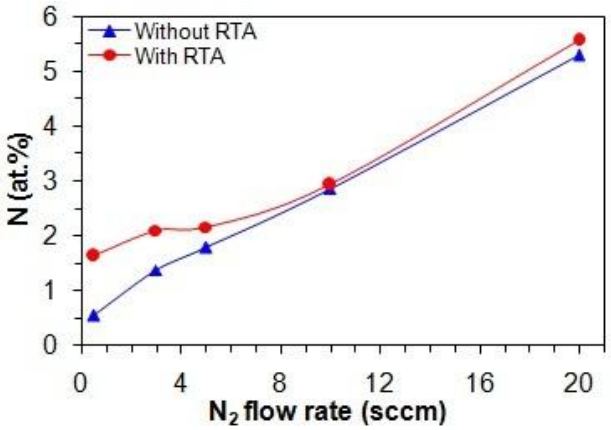


Fig. 1 Surface chemical compositions of taC:N thin films without or with RTA at 200˚C for 2 minutes as a function of N_2 gas flow rate.

The surface N contents of the annealed taC:N thin films with 0.5 and 20 sccm N_2 are 1.63 at.% to 5.56 at.% (3.4 times higher). The surface N contents of the annealed taC:N thin films are 201.9% higher for the 0.5 sccm, 52.6% higher for the 3 sccm, 21.5% higher for the 5 sccm, 2.5% higher for the 10 sccm, and 5.1% higher for the 20 sccm than those of the as-deposited ones. Therefore, it is clear that the increased surface N contents of the annealed taC:N thin films mainly result from the interaction of their surfaces with N species in the vacuum chamber during the annealing process, as the more C-rich surface seems to have more physical or chemical adsorption of N atoms. In addition, the possible diffusion of incorporated N atoms to the film surface during the RTA also contributes to the higher surface N contents of the annealed taC:N thin films compared to those of the as-deposited ones [8,10,11].

The typical XPS C 1s spectra of the as-deposited taC:N thin films with N_2 gas flow rates of 3 sccm and 20 sccm can be found in Figures 2a and 2b, respectively. They have four major peaks: the C-C sp^2 peak at about 284.2 eV, the C-C sp^3 peak at about 285 eV, the C-O peak at about 286 eV, and the C-N peak at about 288.6 eV. The taC:N thin film deposited with 20 sccm N_2 exhibits a significantly higher intensity ratio of C-C sp^2 and C-C sp^3 bonding peaks compared to the 3 sccm N_2 sample. This disparity is attributed to an increased proportion of sp^2-hybridized bonds within the carbon matrix, likely resulting from nitrogen atoms preferentially engaging in π-bonded configurations [1,9,12].

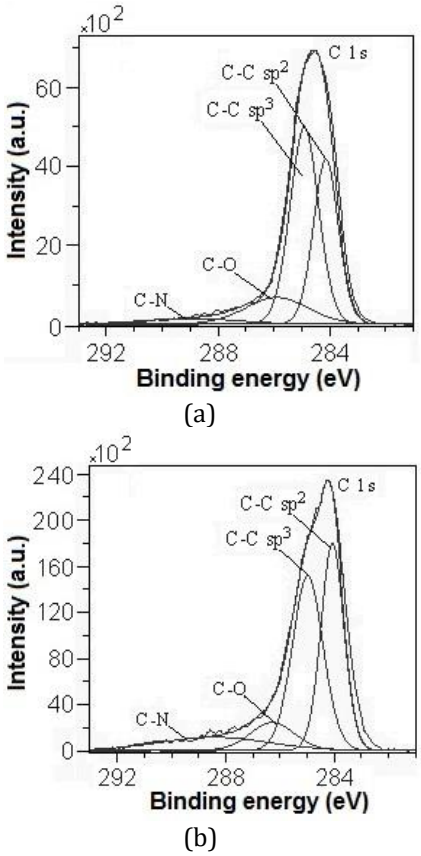


Fig. 2. XPS C 1s spectra of as-deposited taC:N thin films with N_2 gas flow rates of (a) 3 sccm and (b) 20 sccm.

Figure 3 depicts the Raman spectra of as-deposited taC:N thin films synthesized under varying N_2 gas flow rates. In the taC thin films, Raman spectral features primarily arise from sp^2-bonded carbon within their amorphous structure. The observed enhancement in spectral intensities with elevated nitrogen content suggests a corresponding increase in sp^2-hybridized carbon configurations within the matrices, due to nitrogen incorporation promoting sp^2-bond formation. The Raman spectra were fitted with two Gaussian G and D peaks for further analysis.

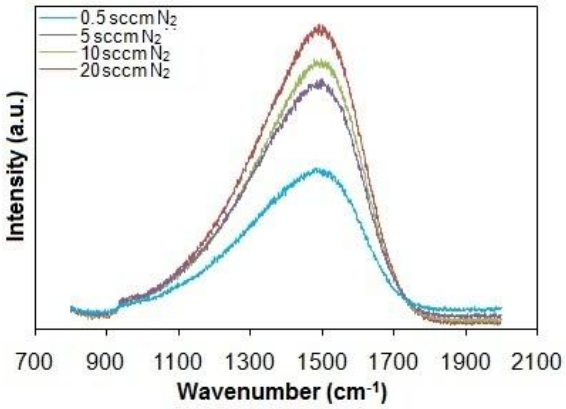


Fig. 3. Raman spectra of as-deposited taC:N thin films with different N_2 gas flow rates.

Figure 4a demonstrates a progressive decrease in the G peak position of as-deposited taC:N thin films, shifting from 1532.3 cm^{-1} to 1528.9 cm^{-1} as the N_2 gas flow rate increases from 0.5 to 20 sccm. Prior studies [1,13] suggest that N doping promotes clustering of sp^2-bonded carbon sites. Elevated N content in taC:N films facilitates the structural reorganization of sp^2-hybridized carbon, transitioning from short-chain configuration to ring formation [1,13–15]. This shift increases the density of ring structures within the carbon matrix. As chain-like bonds possess shorter bond lengths compared to ring structures, the increased number of rings reduces vibrational frequencies in the lattice, thereby downshifting the G peak with higher nitrogen incorporation.

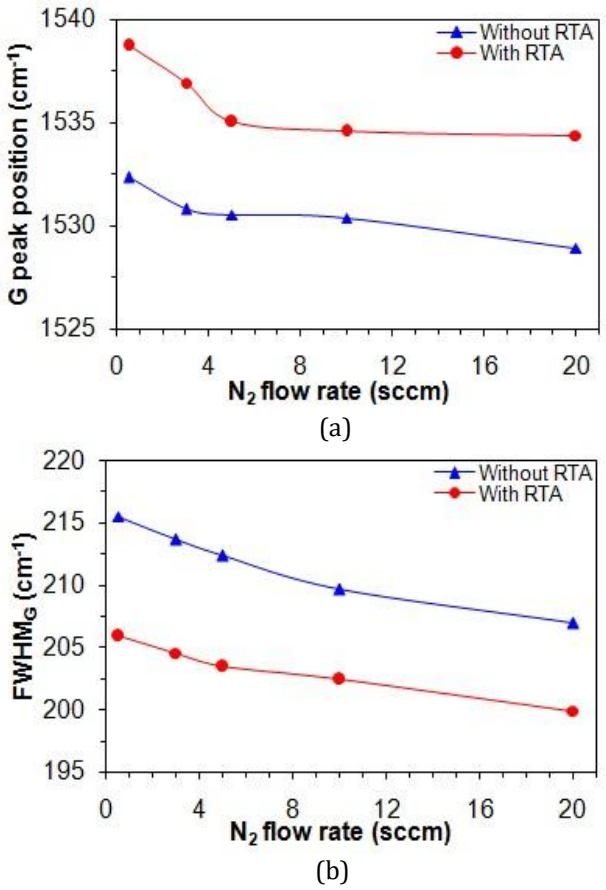


Fig. 4. (a) G peak positions and (b) $FWHMs_G$ of taC:N thin films without or with RTA at 200°C for 2 minutes as a function of N_2 gas flow rate.

It is found that the taC:N thin films show an apparent downshift with an increased N_2 flow rate from 0.5 sccm to 5 sccm and then a slow downshift with a further increased N_2 flow rate to 20 sccm in their G peak positions. It indicates that changes in their amorphous carbon

structures with their N contents are approaching saturation when the N_2 flow rate is increased by more than 5 sccm.

The annealed taC:N thin films exhibit a similar trend of G peak position versus N_2 flow rate to that of the as-deposited ones, which is confirmed by their decreased G peak position from 1538.7 cm^{-1} to 1534.4 cm^{-1} with an increased N_2 gas flow rate from 0.5 sccm to 20 sccm in Figure 4a. However, the G peak positions of the annealed taC:N thin films exist at higher wave numbers for all the N contents compared to those of the as-deposited ones, probably due to the decreased number of tetrahedral bonds and the decreased disorders of bond angles and lengths associated with the annealing [16].

In Figure 4b, the full width-half-at-maximum (FWHM) of the G peaks of the as-deposited taC:N thin films decreases from 215.5 cm^{-1} to 206.9 cm^{-1} with an increased N_2 gas flow rate from 0.5 sccm to 20 sccm, indicating the decreased disorder of rings in their C matrixes with their increased N contents since the disorder of rings contributes to the $FWHM_D$. It also means the increased number of aromatic rings in their C matrixes because N doping encourages sp^2 sites to cluster [5,10]. Similarly, the $FWHM_D$ of the annealed taC:N thin films also decreases from 205.9 cm^{-1} to 199.9 cm^{-1} with an increased N_2 gas flow rate from 0.5 sccm to 20 sccm. However, the $FWHMs_D$ of the annealed taC:N thin films are apparently narrower than those of the as-deposited ones for all the N contents, which can be related to the lowered disorder of rings in their C matrixes associated with the annealing [1,17].

In Figures 5a and 5b, the intensity (I_D/I_G) and area (A_D/A_G) ratios of the D and G peaks of the as-deposited taC:N thin films apparently increase from 0.92 and 1.74 to 1.2 (30.4% increase) and 2.76 (58.6% increase), respectively, with an increased N_2 gas flow rate from 0.5 sccm to 20 sccm. It indicates the increased number of rings per cluster in their C matrixes with their increased N contents as a result of their increased N-induced graphitization. The annealed taC:N thin films also exhibit apparent increases in their I_D/I_G and A_D/A_G ratios from 1.05 and 2.1 to 1.59 (51.4% increase) and 3.29 (64.5% increase), respectively, with an increased N_2 gas flow rate from 0.5 sccm to 20 sccm [9,13].

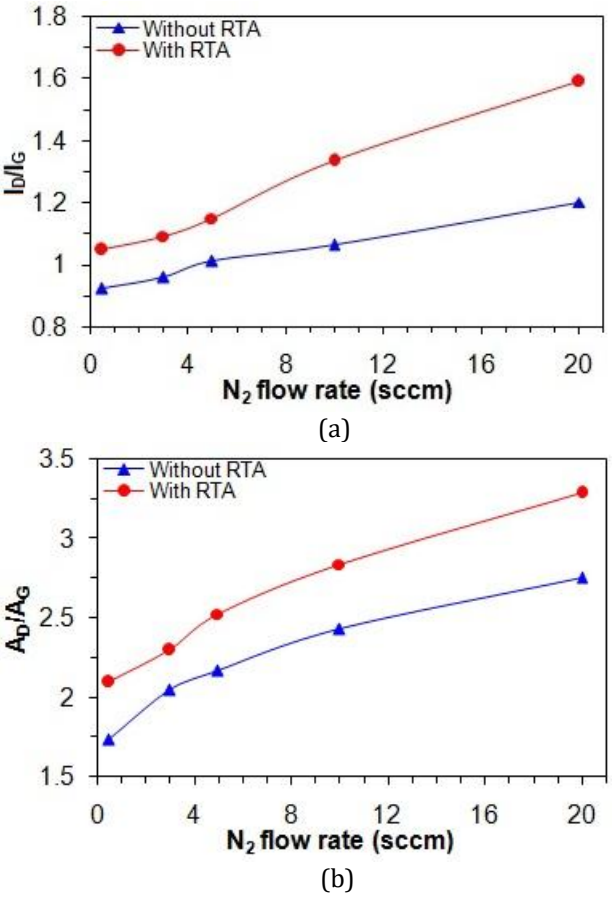


Fig. 5. (a) I_D/I_G and (b) A_D/A_G ratios of taC:N thin films without or with RTA at 200˚C for 2 minutes as a function of N_2 gas flow rate.

The I_D/I_G and A_D/A_G ratios of the annealed taC:N thin films are apparently larger than those of the as-deposited ones for all the N contents, which is indicative of the higher graphitization of their amorphous carbon structures associated with the annealing [17]. A divergence between the trends of I_D/I_G or A_D/A_G versus N_2 gas flow rate of the taC:N thin films without and with the RTA reveals that the annealing causes the higher graphitization of their amorphous carbon structures for their higher N contents via the combined effects of N- and annealing-induced graphitization.

In Figure 6a, the R_a values of the as-deposited taC:N thin films increase from 0.12 nm to 0.23 nm (91.7% increase) with an increased N_2 gas flow rate from 0.5 sccm to 20 sccm. Such an increase in their R_a values can be explained by several factors: increased N-induced graphitization, the increased N aggregation, and reduced film density linked to higher sp^2-bond concentrations [8,9,18]. In Figure 6b, their R_{pm} and R_{vm} values also increase from 0.27 nm and 0.25 nm to 0.45 nm (66.7% increase)

and 0.44 nm (76% increase), respectively, with an increased N_2 gas flow rate from 0.5 sccm to 20 sccm. It reveals that the maximum heights of their surface peaks and the maximum depths of their surface valleys become increased with their increased N contents, which are responsible for their increased surface roughness.

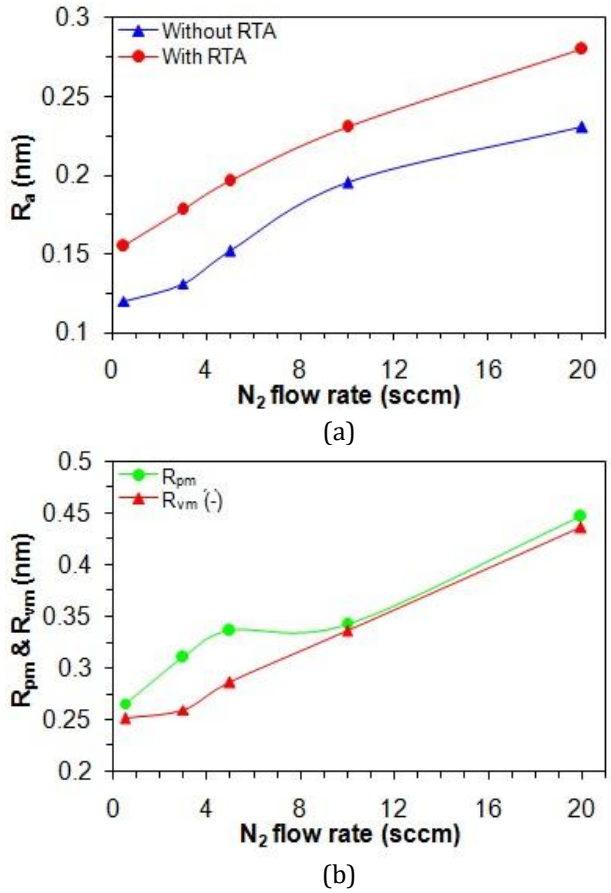


Fig. 6. (a) R_a values of taC:N thin films without or with RTA at 200˚C for 2 minutes as a function of N_2 gas flow rate and (b) R_{pm} and R_{vm} values of taC:N thin films without RTA as a function of N_2 gas flow rate.

The R_a values of the annealed taC:N thin films also increase from 0.16 nm to 0.28 nm (86.7% increase) with an increased N_2 gas flow rate from 0.5 sccm to 20 sccm, as shown in Figure 6a. Their R_a values are apparently larger than those of the as-deposited ones for all the N contents because the annealing further increases their surface roughness by further promoting their graphitization [8,9,17].

Figure 7a shows the surface topography of the as-deposited taC:N thin with 0.5 sccm N_2, on which very fine surface roughness can be found for its relatively smooth surface [19]. In addition, grain-shaped surface waviness can be found, which probably results from a variation in the film density caused by changes in sp^2 and sp^3 contents [19]. The taC:N thin film with a N_2 gas flow rate of 20 sccm has a different surface topography, on which protruded asperities above the surface can be clearly seen, as shown in Figure 7b, which are attributed to N aggregates and graphitic phases in addition to its lower film density with the higher number of sp^2 bonds [8,18,20].

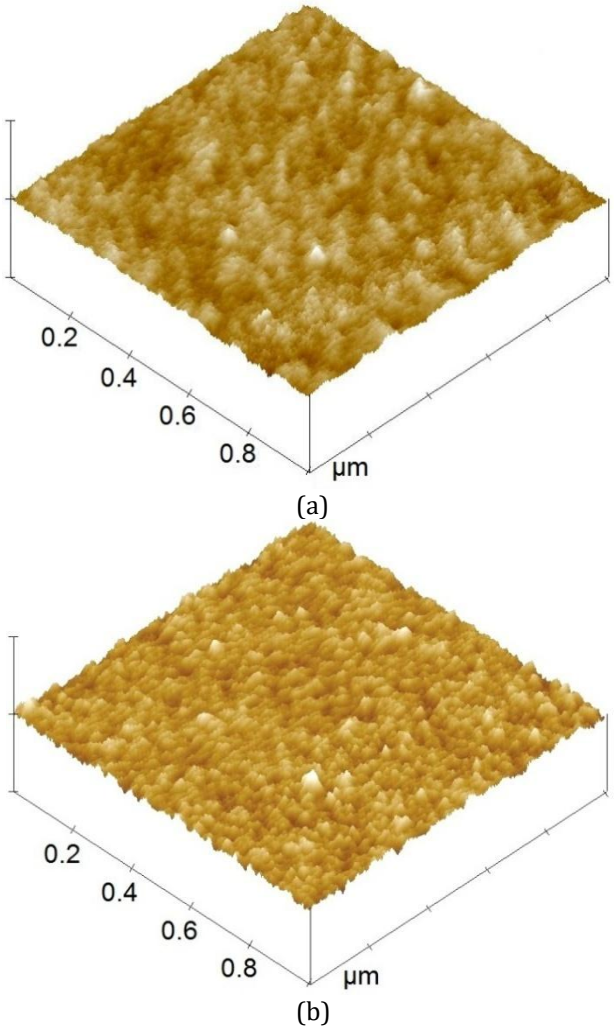


Fig. 7. Surface topographies of taC:N thin films with N_2 gas flow rates of (a and c) 0.5 sccm and (b and d) 20 sccm (a and b) without or (c and d) with RTA at 200 ˚C for 2 minutes. X = 0.2 μm/div, Z = 5 nm/div.

Figure 8 demonstrates an increase in the critical load of as-deposited taC:N thin films, rising from 445 mN to 477.4 mN (a 7.3% enhancement) as the N_2 gas flow rate escalates from 0.5 to 20 sccm. The critical load, defined by a sudden fluctuation in tangential force due to abrupt adhesive failure between the film and substrate [18], reflects the mechanical stability threshold.

As thin films experience immediate mechanical failure at their critical load, the taC:N films in this study show no detectable scratch-induced damage along their tracks prior to reaching their critical load thresholds [21]. It clearly shows that their sp^3 contents are high enough to possess high cohesive strength by forming their rigid sp^3-bonded cross-linking structures and thereby to have a high resistance to scratch-induced damage during the scratching [21].

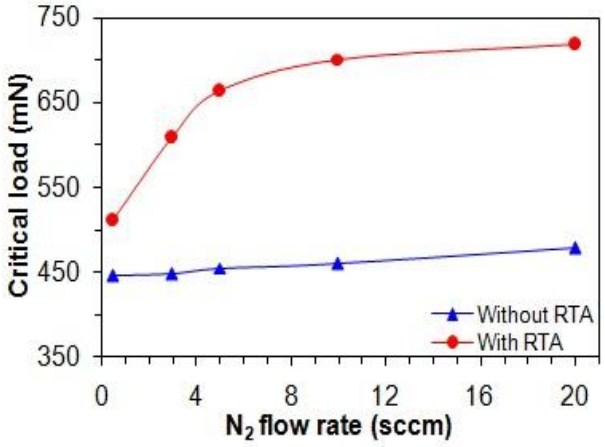


Fig. 8. Critical loads of taC:N thin films without or with RTA at 200°C for 2 minutes as a function of N_2 gas flow rate.

The critical loads of the as-deposited taC:N thin films slightly increase with their increased N contents, indicating their increased adhesion strengths because the critical load results from an interfacial adhesion failure between the film and Si substrate. The elevated residual stress observed in taC films originates from the development of a structurally rigid, sp^3-bonded cross-linking network, so the N doping degrades its network with the increased number of sp^2 bonds, which have a lower coordination number than sp^3 bonds, and N aggregates, reducing the residual stress in its C matrix [1,22]. It is known that sp^2 bonds have shorter bond lengths than sp^3 bonds, as the bond length of chains is shorter as compared to rings [1]. Besides, the bond length of C=N bonds is shorter than those of C-C and C=C bonds [1,22]. Therefore, the increased numbers of sp^2 bonds, C=N bonds, and aromatic rings in the amorphous carbon structures of the taC:N thin films with their increased N contents lead to their decreased residual stress via their structural relaxation and thereby their increased adhesion strength [2,22].

In addition, annealing the taC:N thin film with 0.5 sccm N_2 gives rise to its 14.6% higher critical load of 510 mN compared to that of the as-deposited one with the same N_2 gas flow rate, as shown in Figure 8. The critical load of the annealed taC:N thin film apparently increases to 663.6 mN (30.1% increase) for the increased N_2 gas flow rate of 5 sccm, indicating that the small amount of N atoms in its C matrix greatly helps to improve its adhesion strength during the annealing [23]. However, there is a slowdown in its increased critical load when the N_2 gas flow rate is increased by more than 5 sccm, so that its critical load of 717.8 mN at the N_2 gas flow rate of 20 sccm is 8.2% higher than that of the one with 5 sccm N_2. However, the critical load of the annealed taC:N thin film deposited with 20 sccm N_2 exhibits a 50.4% increase relative to its as-deposited counterpart under identical N_2 flow conditions. It indicates that annealing the taC:N thin films effectively improves their interfacial adhesion strengths for all the N contents [6]. This enhancement is attributed to the annealing process facilitating an increase in sp^2-hybridized carbon bonds within the taC:N matrix through thermally induced graphitization, which in turn degrades their sp^3-bonded cross-linking networks and thereby lowers their residual stress, resulting in their improved adhesion strength [6]. As shown in Figure 8, the observed slowdown in the increased adhesion strength of the annealed taC:N thin films with an increased N content indicates their approaching saturation in their adhesion promotion [23-25].

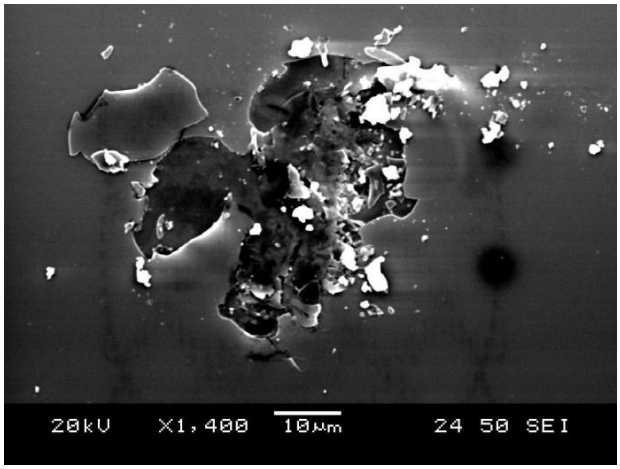


Fig. 9. Scratch-induced damage morphology of as-deposited taC:N thin film with a N_2 gas flow rate of 0.5 sccm observed at its critical load.

Figure 9 shows the scratch-induced damage morphology of the as-deposited taC:N thin film with 0.5 sccm N_2 observed at its critical load, from which a removal of the broken film as a large platelet is found. In addition, small fragments are also found around the damaged area, which suggests that the interfacial adhesion strength of the taC:N thin film surpasses the cohesive strength of the underlying Si substrate, so that minute cracks initiated between the film and substrate at the critical load propagate along the film/substrate interface as well as into the subsurface of the Si substrate to some extent under progressive loading and eventually remove the film and substrate as fragments via their sudden brittle failures.

4. CONCLUSION

The FCVA deposition technique was used to produce the taC:N thin films with different N contents on the Si substrates. Subsequently, they were annealed at the optimized temperature of 200˚C for 2 minutes to investigate the effects of RTA on their structure, surface roughness, and adhesion strength.

- The increased graphitization of the taC:N thin films with their increased N contents or the annealing was found. The annealed taC:N thin films with higher N contents exhibit higher graphitization due to the combined effects of N- and annealing-induced graphitization.
- The surface roughness of the taC:N thin films increased with their increased N contents or the annealing due to the increased numbers of sp^2 bonds, N aggregates, and graphitic phases in their amorphous carbon structures. The annealed taC:N thin films had higher surface roughness than the as-deposited ones for all the N contents due to the annealing-induced graphitization of their amorphous carbon structures.
- The critical loads of the taC:N thin films increased with their increased N contents as a result of their promoted structural relaxation to decrease their residual stress, as further annealing them further improved their adhesion strength. A slowdown in the increased adhesion strength of the annealed taC:N thin films with their increased N contents was found when their N contents were more than 1.78 at.%.
- In conclusion, the N content, or the annealing, had a significant effect on the structure, surface roughness, and adhesion strength of the taC:N thin films.

Acknowledgement

This work was supported by the research grant (EWI-0601-IRIS-035-00) from the Environment & Water Industry Development Council (EWI), Singapore.

REFERENCES

[1] J. Robertson, "Diamond-like carbon amorphous," *Materials Science and Engineering: R: Reports*, vol. 37, iss. 4–6, pp. 129–281, May 2002. doi: 10.1016/S0927-796X(02)00005-0.

[2] D. Bootkul, B. Supsermpol, N. Saenphinit, C. Aramwit, and S. Intarasiri, "Nitrogen doping for adhesion improvement of DLC film deposited on Si substrate by filtered cathodic vacuum arc technique," *Applied Surface Science*, vol. 310, pp. 284-292, Aug. 2014, doi: 10.1016/j.apsusc.2014.03.059.

[3] K. Bewilogua and D. Hofmann, "History of diamond-like carbon films: from first experiments to worldwide applications," *Surface and Coatings Technology*, vol. 242, pp. 214-225, Mar. 2014, doi: 10.1016/j.surfcoat.2014.01.031.

[4] D. R. McKenzie, D. Muller, and B. A. Pailthorpe, "Compressive-stress-induced formation of thin film tetrahedral amorphous carbon," *Physical Review Letters*, vol. 67, iss. 6, pp. 773–776, Aug. 1991, doi: 10.1103/PhysRevLett.67.773.

[5] J. K. Shin, C. S. Lee, K. R. Lee, and K. Y. Eun, "Effect of residual stress on the Raman-spectrum analysis of tetrahedral amorphous carbon films," *Applied Physics Letters*, vol. 78, pp. 631-633, Jan. 2001, doi: 10.1063/1.1343840.

[6] H. Nakazawa, K. Nakamura, H. Osanai, Y. Sasaki, H. Koriyama, Y. Kabayashi, Y. Enta, Y. Suzuki, and M. Suemitsu, "Annealing effects on the properties of hydrogenated diamond-like carbon films doped with silicon and nitrogen," *Diamond and Related Materials*, vol. 122, pp. 108809, Feb. 2022, doi: 10.1016/j.diamond.2021.108809.

[7] B. K. Tay, X. Shi, E. Liu, S. P. Lau, L. K. Cheah, Z. Sun, and J. Shi, "Stress relief of tetrahedral amorphoous carbon films by post-deposition thermal annealing," *Surface and Coatings Technology*, vol. 120-121, pp. 448-452, Nov. 1999, doi: 10.1016/S0257-8972(99)00465-X.

[8] N. W. Khun and E. Liu, "Structures, wettability, and corrosion resistance of annealed platinum/ruthenium/carbon-co-doped diamond-like carbon nanocomposite thin films at different temperatures," *Journal of Materials and Engineering*, vol. 3, iss. 2, pp. 217-229, 2025, doi: 10.61552/JME.2025.02.008.

[9] N. W. Khun and E. Liu, "Nitrogen-induced degradation of corrosion resistance of platinum/ruthenium/nitrogen-doped diamond-like carbon thin films," *Journal of The Electrochemical Society*, vol. 157, no. 8, pp. C269, Jun. 2010, doi: 10.1149/1.3428724.

[10] S. C. Ray, W. Mbiombi, and P. Papakonstantinou, "Diamond-like carbon (DLC) thin films: preparation and characterization," *Applied Mechanics and Materials*, vol. 575, pp. 292–295, Jun. 2014. doi: 10.4028/www.scientific.net/AMM.575.292.

[11] T. F. Zhang, K. W. Kim, and K. H. Kim, "Nitrogen-incorporated hydrogenated amorphous carbon film electrodes on Ti substrates by hybrid deposition technique and annealing," *Journal of The Electrochemical Society*, vol. 163, no. 3, pp. E54, Dec. 2015, doi: 10.1149/2.0051603jes.

[12] J. Hu, P. Yang, and C. M. Lieber, "Nitrogen-driven sp3 to sp2 transformation in carbon nitride materials," *Physical Review B*, vol. 57, iss. 6, pp. R3185, Feb. 1988, doi: 10.1103/PhysRevB.57.R3185.

[13] J. Robertson and C. A. Davis, "Nitrogen doping of tetrahedral amorphous carbon," *Diamond and Related Materials*, vol. 4, iss. 4, pp. 441-444, Apr. 1995, doi: 10.1016/0925-9635(94)05265-4.

[14] T. Kohler, T. Frauenheim, and G. Jungnickel, "Stability, chemical bonding, and vibrational properties of amorphous carbon at different mass densities," Physical Review B, vol. 52, iss. 16, pp. 11837, Oct. 1995, doi: 10.1103/PhysRevB.52.11837.

[15] J. Lee, R. W. Collins, V. S. Veerasamy, and J. Robertson, "Analysis of the ellipsometric spectra of amorphous carbon thin films for evaluation of the sp3-bonded carbon content," *Diamond and Related Materials*, vol. 7, iss. 7, pp. 999-1009, Jul. 1998, doi: 10.1016/S0925-9635(97)00341-5.

[16] D. Beeman, J. Silverman, R. Lynds, and M. R. Anderson, "Modeling studies of amorphous carbon," *Physical Review B*, vol. 30, iss. 2, pp. 870–875, Jul. 1984, doi: 10.1103/PhysRevB.30.870.

[17] W. S. Choi and B. Hong, "The effect of annealing on the properties of diamond-like carbon-protective antireflection coatings," *Renewable Energy*, vol. 33, iss. 2, pp. 226-231, Feb. 2008, doi: 10.1016/j.renene.2007.05.022.

[18] N. W. Khun and E. Liu, "Friction and wear of nitrogen-doped DLC coating and platinum/ruthenium/nitrogen-co-doped DLC nanocomposite coatings," *Journal of Materials and Engineering*, vol. 3, iss. 1, pp. 67–77, 2025, doi: 10.61552/JME.2025.01.004.

[19] C. Casiraghi, A. C. Ferrari, R. Ohr, A. J. Flewitt, D. P. Chu, and J. Robertson, "Dynamic roughening of tetrahedral amorphous carbon," *Physical Review Letters*, vol. 91, iss. 22, pp. 226104, Nov. 2003, doi: 10.1103/PhysRevLett.91.226104.

[20] G. Leal, M. A. Fraga, L. A. Rasia, and M. Massi, "Impact of high N_2 flow ratio on the chemical and morphological characteristics of sputtered N-DLC films," *Surface and Interface Analysis*, vol. 49, iss. 2, pp. 99-106, Feb. 2017, doi: 10.1002/sia.6064.

[21] B. K. Gupta and Bharat Bhushan, "Mechanical properties of amorphous carbon coatings deposited by different deposition techniques," *Thin Solid Films*, vol. 270, iss. 1-2, pp. 391-398, Dec. 1995, doi: 10.1016/0040-6090(95)06699-3.

[22] J. P. Sullivan, T. A. Friedmann, and A. G. Baca, "Stress relaxation and thermal evolution of film properties in amorphous carbon," *Journal of Electronic Materials*, vol. 26, pp. 1021-1029, Sep. 1997, doi: 10.1007/s11664-997-0239-9.

[23] D. S. Grierson, A. V. Sumant, A. R. Konicek, T. A. Friedmann, J. P. Sullivan, and R. W. Carpick, "Thermal stability and rehybridization of carbon bonding in tetrahedral amorphous carbon," *Journal of Applied Physics*, vol. 107, iss. 3, pp. 033523, Feb. 2010, doi: 10.1063/1.3284087.

[24] A. I. Voropaev, V. I. Kolesnikow, O. V. Kudryakov, V. N. Varavka, I. V. Kolesnikov, M. S. Lifar, S. A. Guda, A. A. Guda, and A. V. Sidashov, "Nitrogen-stabilized DLC coatings: optimization of properties and parameters using randomized tree and neural network algorithms," *Physical Mesomechanics*, vol. 27, pp. 355-369, Aug. 2024, doi: 10.1134/S1029959924040015.

[25] J. C. Gamez, S. Shiri, M. Mohammadtaheri, and Q. Yang, "Adhesion enhancement of DLC on CoCrMo alloy by diamond and nitrogen incorporation for wear-resistant applications," *Surface and Coatings Technology*, vol. 332, pp. 120-127, Dec. 2017, doi: 10.1016/j.surfcoat.2017.10.050.